

Resonance Raman scattering by LO phonons in $\text{Cd}_x\text{Hg}_{1-x}\text{Te}$ at the $E_0 + \Delta_0$ gap

José Menéndez and Manuel Cardona

Max-Planck-Institut für Festkörperforschung, Heisenbergstrasse 1, D-7000 Stuttgart 80, Federal Republic of Germany

Lev K. Vodopyanov

*Academy of Sciences of the Union of Soviet Socialist Republics, P. N. Lebedev Physical Institute,
Leninsky Prospect 53, 117924 Moscow, U.S.S.R.*

(Received 12 November 1984)

We have studied the resonance of the first- and second-order Raman scattering by LO phonons in $\text{Cd}_x\text{Hg}_{1-x}\text{Te}$ for $x \approx 1$ near the $E_0 + \Delta_0$ gap. We show that the effect of alloying is a shift and a broadening of the resonances which can be compared with calculations of the compositional dependence of the gaps. The mechanisms contributing to one-LO-phonon and two-LO-phonon scattering are discussed and experimentally investigated. We give absolute values for the Raman efficiencies and compare them with theory.

I. INTRODUCTION

In the last few years, a large number of publications have been devoted to the physics of $\text{Cd}_x\text{Hg}_{1-x}\text{Te}$ substitutional alloys, mainly stimulated by their technological applications as infrared detectors.¹ Optical studies on $\text{Cd}_x\text{Hg}_{1-x}\text{Te}$ can be divided in two groups: those concerned with the electronic structure such as absorption, reflection, and recently ellipsometry,² and those which investigate lattice-dynamical properties, using infrared³⁻⁶ and Raman⁷⁻¹⁰ techniques.

We report in this paper what to our knowledge is the first investigation of resonance Raman scattering (RRS) by phonons in $\text{Cd}_x\text{Hg}_{1-x}\text{Te}$. RRS by phonons provides the link between electronic and lattice-dynamical properties: the energy dependence of the Raman efficiency and its absolute value are determined by the electron-phonon interaction and by parameters of the band structure, such as gap energy, effective masses, and broadening.

RRS by LO phonons is particularly interesting because both short- and long-range parts of the electron-phonon interaction are present. The short-range part can be represented by deformation potentials,¹¹⁻¹³ while the long-range part, the Fröhlich interaction, arises from the electric field generated by LO phonons in polar semiconductors. The deformation potential and the *interband* matrix elements of the Fröhlich interaction lead to a dipole Raman tensor^{11,12} and to the standard selection rules for dipole Raman scattering. However, Raman scattering by LO phonons has been observed near electronic critical points in scattering configurations which are forbidden according to the usual selection rules.¹² This phenomenon occurs for parallel scattered ($\hat{\epsilon}_S$) and incident ($\hat{\epsilon}_I$) light polarizations. For semiconductors at gaps higher than the fundamental one, it has been demonstrated^{14,15} that two mechanisms are responsible for the violation of the dipole selection rules. First, for scattering wave vectors not exactly equal to zero there is a contribution to the Raman tensor—diagonal at three-dimensional critical points—from the *intraband* matrix elements of the Fröhlich in-

teraction.¹⁶ On the other hand, there is an impurity-induced mechanism¹⁷ in which the exciton (the virtual electron-hole pair created by the light in the Raman process) scatters twice, once with the electron-phonon interaction and once with the electron-impurity interaction. This process, of higher (fourth) order in perturbation theory than the intrinsic intraband mechanism, can be of comparable importance because phonons with larger \mathbf{q} vectors are created, enhancing the q -dependent effects of the Fröhlich interaction and producing double-resonance effects.¹⁵

Second-order resonant Raman scattering by LO phonons is mainly due to an iteration of the intraband Fröhlich interaction. The formal theory¹⁸⁻²⁰ is very similar to the impurity-induced one-phonon scattering, with a second phonon interacting formally in the same way as the impurity. Because the enhancement discussed above for impurity-induced one-LO-phonon scattering also takes place here, the contribution of impurity induced two-LO-phonon scattering, which would be at least a fifth order process, can be totally neglected. In other words, whereas impurities affect dramatically the forbidden first-order RRS by LO phonons (induced by the finite but rather small scattering vector), scattering by two LO phonons is only due to the intrinsic intraband Fröhlich mechanism.

The different mechanisms leading to forbidden one- and two-LO-phonon scattering suggest the importance of comparing both resonances measured under the same conditions. Furthermore, in the case of $\text{Cd}_x\text{Hg}_{1-x}\text{Te}$ with x close to 1, like our three samples, the interesting question arises as to what extent the Hg atoms play the role of impurities which induce forbidden LO-phonon scattering. This problem is closely connected with the search for an appropriate description of the band structure of $\text{Cd}_x\text{Hg}_{1-x}\text{Te}$. Different approaches have been used.¹ In the virtual-crystal approximation²¹ (VCA) one solves the problem of an "effective" semiconductor with an average potential for the cation sites. Disorder effects are not taken into account: Within this approximation the only effect to be expected on the Raman spectra is a shift of the

resonances as a function of x following the shift of the electronic gaps. Part of the disorder effects are incorporated in the coherent-potential approximation²² (CPA). In the presence of disorder, the electron wave vector \mathbf{k} ceases to be a good quantum number, and electron states defined by \mathbf{k} are broadened. The broadening of the gap η determines the shape and intensity of the Raman efficiencies (for example, the intensities for impurity-induced LO-phonon scattering or two-LO-phonon scattering are roughly proportional to η^{-2}). Hence, in the CPA, the Raman resonance should shift and change its shape and strength as a function of x . Disorder effects beyond the CPA could manifest themselves in the form of impurity-induced forbidden LO-phonon scattering. This would produce scattering efficiencies for one-LO-phonon scattering which depend explicitly on the concentration x .

We have chosen to work near the $E_0 + \Delta_0$ gap (~ 2.5 eV), between the Γ_6 conduction band and the Γ_7 valence band. This gap lies close to some discrete lines of the cw Ar⁺ laser and can be scanned with commercial dye lasers. On the other hand, the results can be compared with recent studies of forbidden scattering near the $E_0 + \Delta_0$ gap of GaAs.¹⁵ We concentrate our investigation on forbidden LO-phonon and two-LO-phonon scattering. The results are qualitatively in agreement with the CPA. No correlation has been found between the Hg concentration and the intensities for forbidden one-LO-phonon scattering beyond the predictions of the CPA theory.

II. EXPERIMENTAL

Samples were grown by R. Triboulet with the traveling heater method.²³ They are p type with a carrier concentration of $p \sim 10^{16}$ cm⁻³. Slabs of different compositions ($x = 1, 0.966, \text{ and } 0.944$) oriented in the $[1\bar{1}0]$ direction were polished with Syton and etched with a Br-methanol solution. The samples were glued to the cold finger of an N₂ cryostat together with a silicon crystal which was used as a scattering reference. The temperature for all measurements was 100 K. The $E_0 + \Delta_0$ gap of all three Cd _{x} Hg _{$1-x$} Te samples are inside the lasing region of the Coumarin 30 dye (Coherent, Inc). This dye was pumped with all violet lines of a cw Kr⁺ laser. The laser beam was focused with a cylindrical lens onto the samples. The power density was kept below 10 W/cm². The detection optics consisted of a Jarrel-Ash 1-m double monochromator equipped with holographic gratings and an RCA 31034 photomultiplier. Data were stored in a multichannel analyzer and subsequently transferred to a computer.

We worked in a backscattering configuration at the $(1\bar{1}0)$ face with both incident ($\hat{\mathbf{e}}_L$) and scattered ($\hat{\mathbf{e}}_S$) polarizations parallel to $[112]$. For this configuration one-LO-phonon scattering is forbidden according to the dipole selection rules. Hence, we can only observe the two mechanisms mentioned in Sec. I which lead to a violation of the usual selection rules. Note that for this scattering configuration it is not possible to observe the interference effects reported in Refs. 14 and 15, because Raman scattering by LO phonons is forbidden by the dipole selection rules for backscattering at $[1\bar{1}0]$.¹²

The scattering efficiency for LO phonons is defined as²⁴

$$\left. \frac{dS}{d\Omega} \right|_{\text{LO}} = \frac{1}{V} \left[\frac{d\sigma_{\text{LO}}}{d\Omega} \right] = \frac{\hbar\omega_L\omega_S^3\eta_S}{2c^4\Omega_{\text{LO}}n_L} |\hat{\mathbf{e}}_S \cdot \vec{\chi}''_{\text{LO}} \cdot \hat{\mathbf{e}}_L|^2 [n(\Omega_{\text{LO}}) + 1], \quad (1)$$

where V is the scattering volume, Ω_{LO} the phonon frequency, ω_L (ω_S) the incident (scattered) photon frequency, n_L and n_S the corresponding indices of refraction, $\hat{\mathbf{e}}_S$ and $\hat{\mathbf{e}}_L$ the light polarization vectors (electric field), $n(\Omega_{\text{LO}})$ the phonon occupation factor, c the speed of light in vacuum, and $\vec{\chi}''$ the volume-independent Raman susceptibility.^{12,24}

An analogous definition can be used for two-LO-phonon (2LO) scattering:

$$\left. \frac{\partial S}{\partial \Omega} \right|_{2\text{LO}} = \frac{\hbar^2\omega_L\omega_S^3\eta_S}{4c^4\Omega_{\text{LO}}^2\eta_L} |\hat{\mathbf{e}}_S \cdot \vec{\chi}''_{2\text{LO}} \cdot \hat{\mathbf{e}}_L|^2 [n(\Omega_{\text{LO}}) + 1]^2. \quad (2)$$

Both Raman susceptibilities in Eqs. (1) and (2) are diagonal tensors for the process near the $E_0 + \Delta_0$ gap discussed in this paper: forbidden LO-phonon Raman scattering,^{12,15} and two-LO-phonon scattering by iteration of the intraband Fröhlich interaction.¹⁸

In Ref. 15 we have written our Raman efficiencies in terms of the polarizability tensor $\vec{\mathbf{R}}$, whose independent components α are related to the independent components of $\vec{\chi}''$ by

$$\chi''_{\text{LO}} = \left[\frac{1}{v_c M^*} \right]^{1/2} \alpha_{\text{LO}}, \quad (3)$$

where v_c is the unit-cell volume and M^* its reduced mass. In this work, however, we shall give our results in terms of the Raman efficiencies themselves, which are more convenient in order to compare first- and second-order scattering. The measured scattering rate *outside* the sample is related to the scattering efficiency by²⁴

$$\frac{\partial R_S}{\partial \Omega'} = \left[\frac{P'_L T_S T_L}{(\alpha_L + \alpha_S) n_S^2 \hbar\omega_L} \right] \frac{\partial S}{\partial \Omega}. \quad (4)$$

Here, P'_L is the incident power, T_S and T_L the power transmission coefficients ($T = 1 - r$, where r is the reflectivity), α_L and α_S the absorption coefficients, and $d\Omega'$ is the solid angle for collection outside the crystal.

The curly bracket in Eq. (4) has to be used as a correction factor to obtain the Raman efficiencies in terms of the measured scattering rates. We use the sample substitution method,¹² whereby we compare the scattering rates of the Cd _{x} Hg _{$1-x$} Te samples with a reference sample of known Raman efficiency. We use silicon as a reference. Near $\hbar\omega_L = 2.5$ eV, the Raman efficiency of Si can be approximated by²⁵

$$\frac{\partial S}{\partial \Omega} (\text{sr}^{-1} \text{cm}^{-1}) = 3.1 \times 10^{-5} / [\hbar\omega(\text{eV}) - 3.4]^4.$$

The absorption coefficients, reflectivity and refractive indices for the Cd _{x} Hg _{$1-x$} Te samples were obtained from

the ellipsometric data of Viña *et al.*², correcting for the temperature shift. Absorption data for Si were taken from Dash and Newman,²⁶ and the refraction index and reflectivity from Aspnes and Studna.²⁷

III. RESULTS

A typical spectrum for $\text{Cd}_{0.966}\text{Hg}_{0.034}\text{Te}$ is shown in Fig. 1 for the 5017-Å line of the Ar^+ laser. The enhanced one- and two-LO-phonon peaks are much stronger than any other observed structures⁷⁻¹⁰ which appear as a background near the $E_0 + \Delta_0$ resonance.

The scattering efficiencies for $\text{Cd}_x\text{Hg}_{1-x}\text{Te}$ can be determined from the known Raman efficiency of silicon by using Eq. (4). The ratio between the scattering rates for Si and $\text{Cd}_x\text{Hg}_{1-x}\text{Te}$ is obtained from the areas of the respective Raman peaks.

The quantities $(\partial S/\partial \Omega)_{\text{LO}}$ and $(\partial S/\partial \Omega)_{2\text{LO}}$ are shown in Figs. 2 and 3, respectively. Note that the resonances shift to lower energy with decreasing x , as one would expect for a continuous transition from CdTe to HgTe. There is also an increment of the broadening and a reduction of the efficiencies as a function of the Hg concentration. However, the two-LO-phonon and one-LO-phonon spectra are not affected in the same way.

An important characteristic of the spectra is the relative shift of the one- and two-LO-phonon resonances for a given sample. We show in Table I the quantity

$$\alpha = [\hbar\omega_{\text{max}}(2\text{LO}) - \hbar\omega_{\text{max}}(\text{LO})] / \hbar\Omega_{\text{LO}},$$

the difference between the maxima in both resonances divided by the phonon frequencies. The reason why α is of the order of one will be discussed in the next sections.

IV. THEORY

A. Forbidden one-LO-phonon Raman scattering

The theory of forbidden one-LO-phonon scattering has been reviewed in Ref. 12 and more recently in Ref. 15 for the specific case of the $E_0 + \Delta_0$ gap of GaAs. We consid-

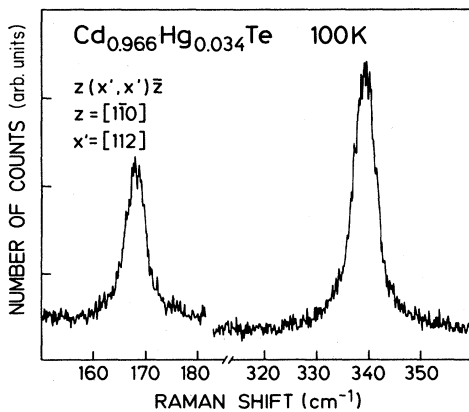


FIG. 1. Raman spectrum of $\text{Cd}_{0.966}\text{Hg}_{0.034}\text{Te}$. The laser wavelength is $\lambda_L = 5017 \text{ \AA}$.

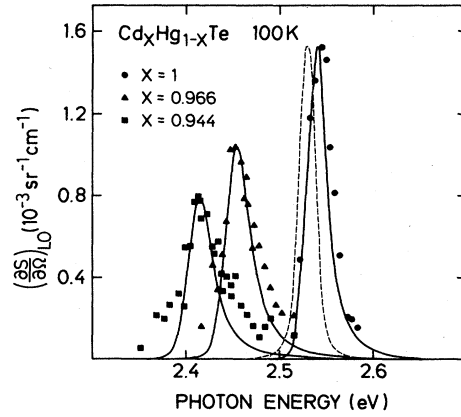


FIG. 2. Experimental scattering efficiencies for first-order Raman scattering by LO phonons in $\text{Cd}_x\text{Hg}_{1-x}\text{Te}$ (forbidden configuration). Solid lines are fits assuming impurity-induced scattering. The dashed line represents the LO phonon resonance for the case of intrinsic forbidden LO phonon scattering. See discussion in text.

er two scattering mechanisms: an "intrinsic" one, involving intraband matrix elements of the Fröhlich interaction, and an impurity-induced mechanism.

1. Intrinsic forbidden LO-phonon scattering

The Raman susceptibility near $E_0 + \Delta_0$ is a diagonal tensor whose independent component, neglecting excitonic effects, is given by¹²

$$\chi''_{\text{LO}} = \frac{q}{12\pi} \left[\frac{e}{m\hbar} \right]^2 \frac{C_F}{\hbar\Omega_{\text{LO}}} \left[\frac{1}{\omega_L} \right]^2 \left[\frac{\omega_L}{\omega_S} \right]^{1/2} \times (4\mu)^{1/2} \left[\frac{2P^2}{3} \right] (s_e - s_h) F(\omega_L), \quad (5)$$

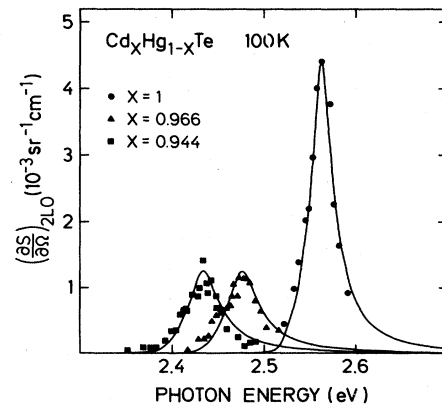


FIG. 3. Experimental scattering efficiencies for second-order Raman scattering by LO phonons in $\text{Cd}_x\text{Hg}_{1-x}\text{Te}$. Solid lines are fits with an expression proportional to Eq. (7).

TABLE I. Energy separation between the resonant maxima in two- and one-LO-phonon Raman scattering normalized to the phonon energy, for three samples of $\text{Cd}_x\text{Hg}_{1-x}\text{Te}$.

x	$\alpha = [\hbar\omega_{\max}(2\text{LO}) - \hbar\omega_{\max}(\text{LO})] / \hbar\Omega_{\text{LO}}$
1.00	1.04
0.966	0.89
0.944	1.04

where \mathbf{q} is the wave vector of the created phonon, e and m are the free-electron charge and mass, $\mu^{-1} = m_e^{-1} + m_h^{-1}$; $s_{e,h} = m_{e,h} / (m_e + m_h)$, with m_e (m_h) being the electron (hole) effective masses. C_F is the Fröhlich constant $C_F = [2\pi e^2(1/\epsilon_\infty - 1/\epsilon_0)\hbar\Omega_{\text{LO}}]^{1/2}$. P is the momentum matrix element $\langle x | p_x | s \rangle = -iP$, and the function $F(\omega_L)$ is given by

$$F(\omega_L) = \left[\left(\frac{\hbar\omega_L - E_g + i\eta}{\hbar\Omega_{\text{LO}}} \right)^{1/2} - \left(\frac{\hbar\omega_S - E_g + i\eta}{\hbar\Omega_{\text{LO}}} \right)^{1/2} \right]^3. \quad (6)$$

$$|\chi''_{2\text{LO}}|^2 = \frac{1}{4} \left[\frac{1}{2\pi} \right]^8 \left[\frac{1}{\omega_L \omega_S} \right]^2 \left[\frac{\omega_S}{\omega_L} \right] \left[\frac{e}{m} \right]^4 \left[\frac{2P^2}{3} \right]^2 \frac{1}{\hbar^4} \frac{1}{(\hbar\Omega_{\text{LO}})^4} \frac{C_F^4}{(a^*)^5} \\ \times \int_0^\infty \frac{dx}{x^2} |A(s_e x, -s_e x, x_1, x_2, x_3) + A(s_h x, -s_h x, x_1, x_2, x_3) \\ - A(s_e x, s_h x, x_1, x_2, x_3) - A(s_h x, s_e x, x_1, x_2, x_3)|^2. \quad (7)$$

Here the parameter a^* is given by $(a^*)^2 = \hbar^2 / (2\mu\hbar\Omega_{\text{LO}})$. The function A is defined in Ref. 18. The maximum of $(\partial S / \partial \Omega)_{2\text{LO}}$ takes place for $\hbar\omega_L = E_g + 2\hbar\Omega_{\text{LO}}$. The reason is also to be found in the double resonance mentioned above for the case of impurity-induced forbidden scattering. We suspect that there is a mistake in Fig. 1 of Ref. 16, showing the maximum at $\hbar\omega = E_g + \hbar\Omega_{\text{LO}}$. This mistake has led Bechstedt and Haus²⁸ to the erroneous conclusion that excitonic effects are needed to explain resonances at $\hbar\omega_L = E_g + 2\hbar\Omega_{\text{LO}}$. We point out that some puzzling instances in the literature concerning the position of the resonance peaks for forbidden LO scattering and for two-phonon scattering can be easily explained in the manner just discussed.^{29,30}

V. COMPARISON WITH EXPERIMENT

A first indication that the forbidden one-LO-phonon scattering is not due to the intrinsic mechanism but to the

Here the imaginary parts of the square roots are to be taken as positive. E_g is the gap energy. The quantity $(\partial S / \partial \Omega)_{\text{LO}} \propto |\chi''_{\text{LO}}|^2$ peaks at $\hbar\omega_L = E_g + \hbar\Omega_{\text{LO}}/2$, i.e., half way between the ingoing and outgoing resonances.

2. Impurity-induced forbidden LO-phonon scattering

As discussed in Ref. 15, this process is of fourth order in perturbation theory. The virtual electron-hole pair created by the light is scattered by the electron-phonon and by the electron-impurity interaction. We assume ionized impurities with an interacting potential¹⁵ $V(\mathbf{q}) = 4\pi e^2 / \epsilon_0 (q^2 + q_F^2)$, where $q_F = 2/\lambda$, λ being the mean distance between impurities. The expression for a_{LO} [which can be written in terms of χ''_{LO} by using Eq. (3)] is given in the Appendix to Ref. 15. The scattering efficiency has a maximum for $\hbar\omega_L \approx E_g + \hbar\Omega_{\text{LO}}$ (outgoing resonance), in contrast with the intrinsic case. This is due to the fact that when the outgoing photon energy $\hbar\omega_S$ equals the gap, the energy $\hbar(\omega_L - \Omega_{\text{LO}})$ lies in the continuum of excitations and hence a double resonance occurs.

B. Raman scattering by two LO phonons

A number of calculations has been published,¹⁷⁻¹⁹ assuming that the dominant contribution is given by an iteration of the intraband Fröhlich interaction. Using our definition of the Raman susceptibility, the result of Zeyher can be written

impurity effect, can be obtained by comparing the values of the separations between the resonance maxima (Table I) with the theoretical predictions. According to Eq. (5), for intrinsic forbidden one-LO-phonon scattering one expects a maximum at $\hbar\omega_L = E_g + \hbar\Omega_{\text{LO}}/2$. The same theory predicts the maximum at $\hbar\omega_L = E_g + 2\hbar\Omega_{\text{LO}}$ for two-LO-phonon scattering. This means that for intrinsic first-order scattering, the parameter α should be $\alpha \approx 1.5$. The experimental value $\alpha \approx 1$ suggests the dominance of impurity-induced scattering: In this case, $(\partial S / \partial \Omega)_{\text{LO}}$ peaks near $E_g + \hbar\Omega_{\text{LO}}$. This would explain the value $\alpha \approx 1$ obtained experimentally.

The gap position E_g and the corresponding broadening η are parameters of the calculation. A good theory should be able to fit simultaneously the one- and two-LO-phonon resonances using the same set of parameters. Furthermore, η should give a good fit of the resonance shape and be such that the theoretical absolute values for the Raman efficiencies are comparable with experiment.

A. Two-LO-phonon Raman scattering

As only one mechanism is involved in this process, it is natural to begin with its discussion. We have fitted the three curves in Fig. 3 with an expression *proportional* to Eq. (7), using E_g and η as parameters. The fits are the solid lines in Fig. 3. The obtained values of E_g (i.e., $E_0 + \Delta_0$) are shown in Fig. 4. The broadening parameter found from the fit is $\eta = 6$ meV for CdTe and $\eta = 11$ meV for $x = 0.966, 0.944$. See that the η parameter fits simultaneously the shape and the *relative* intensity of the two-LO-phonon resonances: *No scaling factor has been introduced between the three curves.* Having determined E_g and η , we can now estimate the absolute values of $(\partial S/\partial \Omega)_{2\text{LO}}$ at the maximum of the resonance and compare them with experiment. The value obtained for CdTe, using the parameters of Table II, is $(\partial S/\partial \Omega)_{2\text{LO}} = 7.0 \times 10^{-4} \text{ sr}^{-1} \text{ cm}^{-1}$. The experimental value from Fig. 3 is $(\partial S/\partial \Omega)_{2\text{LO}} = 4.3 \times 10^{-3} \text{ sr}^{-1} \text{ cm}^{-1}$. The qualitative agreement obtained can be considered as satisfactory in view of the experimental error, uncertainties in the parameters of the calculation, and the neglect of excitonic enhancement in the theory. We have previously shown¹⁵ that excitonic effects play only a small role at $E_0 + \Delta_0$ in GaAs. However, stronger effects are expected in the II-VI compounds where the lattice screening is smaller and the masses larger.

B. One-LO-phonon Raman scattering

If we assume that the one-phonon scattering is due to the intrinsic intraband Fröhlich mechanism and attempt to fit the one-LO-phonon resonance with the set of parameters $\{E_g, \eta\}$ determined from the two-LO-phonon resonance using Eq. (7), we cannot obtain good agreement with experiment. The curve for CdTe is shown as a dashed line in Fig. 2. It is clear that neither the resonance position nor the resonance shape (in particular the tail to higher energies) are well reproduced by the theory. Furth-

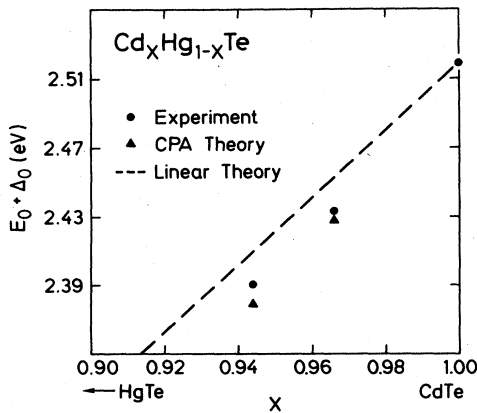


FIG. 4. Compositional dependence of the $E_0 + \Delta_0$ gap in $\text{Cd}_x\text{Hg}_{1-x}\text{Te}$: circles, Raman data; triangles, CPA theory. The dashed line is a linear extrapolation, equivalent to VCA theory.

TABLE II. CdTe parameters used to evaluate the theoretical Raman efficiencies.

$\Omega_{\text{LO}} = 173 \text{ cm}^{-1}$	$m_e = 0.11m^a$
$M^* = 1.088 \times 10^5 m$	$m_h = 0.26m^b$
$a_0 = 6.481 \text{ \AA}$	$P^2/m = 12.52 \text{ eV}^c$
$q = 8.37 \times 10^{-3} \text{ \AA}^{-1}$	$q_F a = 1.4$

^aD. T. F. Marple, Phys. Rev. **129**, 2466 (1963).

^bFit to theoretical calculation of the band structure [H. Overhof, Phys. Status Solidi **45**, 315 (1971)]. The same value is obtained from $\mathbf{k}\cdot\mathbf{p}$ theory: M. Cardona, J. Phys. Chem. Solids **24**, 1543 (1963).

^cM. Cardona, J. Phys. Chem. Solids **24**, 1543 (1963).

ermore, replacing values in Eqs. (2) and (5), we obtain $(\partial S/\partial \Omega)_{\text{LO}} = 1.1 \times 10^{-6} \text{ sr}^{-1} \text{ cm}^{-1}$, which is much smaller than the experimental value of $(\partial S/\partial \Omega)_{\text{LO}} = 1.6 \times 10^{-3} \text{ sr}^{-1} \text{ cm}^{-1}$.

The discrepancy between theory and experiment is a factor of 1400 whereas for the two-LO-phonon case the discrepancy corresponded only to a factor of 6. Bearing in mind that both calculations are based on the same theory, the two-LO-phonon expression being just an iteration of the Fröhlich Hamiltonian, we must conjecture that some mechanism associated with impurities gives the dominant contribution to one-LO-phonon scattering.

We try to fit our one-LO-phonon resonances using the theory for one-LO-phonon scattering induced by ionic impurities described in Sec. IV and in detail in Ref. 15. The total impurity concentration is not known. We use $N_A + N_D \approx 10^{17} \text{ cm}^{-3}$, which may be a reasonable number for a sample with $p \approx 10^{16} \text{ cm}^{-3}$. Possible charged impurities in $\text{Cd}_x\text{Hg}_{1-x}\text{Te}$ are listed in Ref. 1.

We recall that the electron-impurity interaction was assumed to be of the type $4\pi e^2/[\epsilon_0(q^2 + q_F^2)]$ (see Sec. IV). The parameter q_F is taken to be $2/\lambda$, where λ is the mean distance between impurities. In the case of GaAs discussed in Ref. 15, the impurity concentration is so low that q_F happens to be much smaller than those phonon wave vectors which contribute significantly to the Raman scattering. Hence the parameter q_F does not play any role in the position and absolute values of the resonance. In the case of $\text{Cd}_x\text{Hg}_{1-x}\text{Te}$, with the assumed total impurity concentration of 10^{17} cm^{-3} , q_F becomes comparable with the relevant phonon wave vectors. The effect is a shift of the resonance peak to higher energies closer to $E_g + \hbar\Omega_{\text{LO}}$ and a reduction of the absolute values.

The fits obtained using the $\{E_g, \eta\}$ values obtained from the two-LO-phonon resonance are shown as solid lines in Fig. 2. The improvement over the "intrinsic" theory is apparent. The curves for the samples with $x = 0.966, 0.944$ have been multiplied by an additional factor close to 2, which may mean that the impurity concentration should be slightly higher. For the absolute values, we obtain in the case of CdTe, using the expression given in Ref. 15, $(\partial S/\partial \Omega)_{\text{LO}} = 8.4 \times 10^{-4} \text{ sr}^{-1} \text{ cm}^{-1}$, which compares well with the experimental value $1.6 \times 10^{-3} \text{ sr}^{-1} \text{ cm}^{-1}$.

The fit to the one-LO-phonon resonances could be even improved if one uses a somewhat larger broadening pa-

parameter, which would not affect dramatically the quality of the two-LO-phonon fit. However, we have preferred to keep the values obtained from the best fit to the two-LO-phonon resonance, because of the possibility of having some contribution of allowed LO scattering away from the resonance maximum, due to small misorientations of the samples.

We indicated above that in order to fit the one-LO-phonon resonances for the samples containing Hg, we may assume a higher impurity concentration than in our CdTe sample. There is, however, no evidence that these impurities are related to the Hg content itself. In any case, Hg does not play a dominant role as an impurity in one-LO-phonon RRS since the scattering efficiency is also mainly impurity induced in the pure CdTe case. Furthermore, comparing the two samples containing Hg, we see that the sample with the highest Hg concentration has the weakest one-LO-phonon resonance. We therefore conclude that there is no evidence of a correlation between Hg content and RRS beyond the CPA approximation and that the forbidden one-LO-phonon scattering is produced by extrinsic impurities. The possible reason for this is that a charged impurity produces a much larger perturbation than the replacement of the Cd atom by an isoelectronic Hg atom. This can be seen by comparing the huge shifts produced by ionic impurities in the gap energies of Si (Ref. 31) with the few millivolts shift produced in CdTe by much higher concentrations of Hg.

C. Band-structure parameters

The set of parameters $\{E_g, \eta\}$ obtained for each concentration x can be compared with theoretical predictions. In Fig. 4 we show the experimental values of the gap energy, together with the prediction of two theoretical approaches. Both theoretical curves have been obtained by neglecting the x dependence of the spin-orbit parameter Δ_0 in the range $x=0.94-1.00$. The change of Δ_0 between $x=0.944$ and 1.0 can be estimated to be less than 5 meV.³² The dashed line in Fig. 4 represents a linear interpolation of the gap between CdTe and HgTe. It should nearly equal the VCA gap because this theory predicts only a very small quadratic term in the composition dependence of the gap.² Triangles represent the CPA calculation (Fig. 6 of Ref. 22) shifted so as to fit the measured $E_0 + \Delta_0$ gap for CdTe. Figure 4 shows that our points are closer to the CPA predictions than to the VCA approximation.

The effect of disorder is neglected in the VCA approximation. Hence the broadening η depends only on the electron-phonon interaction and the VCA predicts essentially the same broadening for our three samples. Our RRS results show however a larger η for the samples with Hg: $\eta=11$ meV for $x=0.966, 0.944$ and $\eta=6$ meV for CdTe. Possible differences between the two samples with Hg content are within experimental error, which for $\eta=11$ meV is of the order of 3 meV. If we assume that phonon and disorder broadening add, we are left with a disorder broadening of 5 meV. This value is lower than that obtained by extrapolating [as $x(1-x)$] the results of Ref. 20 for $\text{Cd}_{0.7}\text{Hg}_{0.3}\text{Te}$. With this extrapolation we obtain 9 and 15 meV for the disorder-induced broadening in the $x=0.966$ and 0.944 samples, respectively. We should stress, however, that an $x(1-x)$ dependence of the broadening is by no means obvious. This dependence is a trivial consequence of second-order perturbation theory,³³ but within this scheme the broadening at the Γ point in the conduction band should be zero, because there is no density of states to decay into. The CPA theory, however, predicts a broadening at Γ_6 which for $\text{Cd}_{0.7}\text{Hg}_{0.3}\text{Te}$ is comparable with the broadening at Γ_7 . Hence, the Γ point broadening cannot be described by second-order perturbation theory and the extrapolation made above could be erroneous. Furthermore, the CPA calculation²² shows that the E_0 gap energy *does not* follow the $x(1-x)$ law.

VI. CONCLUSIONS

We have presented RRS data for $\text{Cd}_x\text{Hg}_{1-x}\text{Te}$ and shown the importance of comparing one- and two-LO-phonon resonances in order to analyze the different mechanisms involved in both processes. We have shown evidence that first-order forbidden RRS by LO phonons is induced by charged impurities, confirming the suggestion^{15,17} that the intrinsic intraband Fröhlich mechanism is only important for extremely pure samples. We show that the Hg atoms in $\text{Cd}_x\text{Hg}_{1-x}\text{Te}$ for $x \approx 1$ do not act as impurities which induce RRS by LO phonons, probably due to the nonionic character of the perturbation.

ACKNOWLEDGMENTS

We gratefully acknowledge the technical assistance of M. Siemers, P. Wurster, and H. Hirt. One of us (L.K.V.) wishes to acknowledge the warm hospitality experienced at the Max-Planck-Institut.

¹For an updated review on $\text{Cd}_x\text{Hg}_{1-x}\text{Te}$, see R. Dornhaus and G. Nimtz, in *Narrow Gap Semiconductors*, Vol. 98 of *Springer Tracts in Modern Physics*, edited by G. Höhler (Springer, Berlin, 1983), p. 119.

²L. Viña, C. Umbach, M. Cardona, and L. Vodopyanov, *Phys. Rev. B* **29**, 6752 (1984), and references therein.

³M. Hodet, P. Plumelle, M. Vandevyver, R. Triboulet, and Y. Marfaing, *Phys. Status Solidi B* **92**, 545 (1979).

⁴D. N. Talwar and M. Vandevyver, *J. Appl. Phys.* **56**, 1601 (1984).

⁵S. C. Shen, J. H. Chu, and H. J. Ye, in *Proceedings of the International Conference on the Physics of Semiconductors*, San Francisco, 1984, edited by W. Harrison (unpublished).

ternational Conference on the Physics of Semiconductors, San Francisco, 1984, edited by W. Harrison (unpublished).

⁶S. P. Kozyrev, L. K. Vodopyanov, and R. Triboulet, *Solid State Commun.* **45**, 383 (1983).

⁷A. Mooradian and T. C. Harman, in *The Physics of Semimetals and Narrow Gap Semiconductors*, edited by D. L. Carter and R. T. Bate (Pergamon, Oxford, 1971).

⁸P. M. Amirtharaj, K. K. Tiong, and F. H. Pollak, *J. Vac. Sci. Technol. A* **1**, 1744 (1983).

⁹K. K. Tiong, P. M. Amirtharaj, P. Parayanthal, and F. H. Pollak, *Solid State Commun.* **50**, 891 (1984).

- ¹⁰P. M. Amirtharaj, K. K. Tiong, P. Parayanthal, and F. H. Pollak, in Proceedings of the International Conference on the Physics of Semiconductors, San Francisco, 1984, Ref. 5; L. K. Vodopyanov, S. P. Kozyrev, Yu. A. Aleshchenko, R. Triboulet, in Ref. 5.
- ¹¹W. Richter, in *Solid State Physics*, Vol. 78 of *Springer Tracts in Modern Physics*, edited by G. Höhler (Springer, Berlin, 1976), p. 121.
- ¹²M. Cardona, in *Light Scattering in Solids II*, Vol. 50 of *Topics in Applied Physics*, edited by M. Cardona and G. Güntherodt (Springer, Berlin, 1982), p. 19.
- ¹³P. Vogl, in *Physics of Nonlinear Transport in Semiconductors*, edited by D. K. Ferry, J. R. Barker, and C. Jacoboni (Plenum, New York, 1980).
- ¹⁴J. Menéndez and M. Cardona, *Phys. Rev. Lett.* **51**, 1297 (1983).
- ¹⁵J. Menéndez and M. Cardona, preceding paper, *Phys. Rev. B* **31**, 3696 (1985).
- ¹⁶D. C. Hamilton, *Phys. Rev.* **188**, 1221 (1969).
- ¹⁷A. A. Gogolin and E. I. Rashba, *Solid State Commun.* **19**, 1177 (1976).
- ¹⁸R. Zeyher, *Phys. Rev. B* **9**, 4439 (1974).
- ¹⁹A. A. Abdumalikov and A. A. Klochikhin, *Phys. Status Solidi B* **80**, 43 (1977).
- ²⁰A. A. Klyuchikhin, S. A. Permogorov, and A. N. Reznitskii, *Zh. Eksp. Teor. Fiz.* **71**, 2230 (1976) [*Sov. Phys.—JETP* **44**, 1176 (1976)].
- ²¹See, for example, D. J. Chadi and M. L. Cohen, *Phys. Rev. B* **7**, 692 (1973).
- ²²K. C. Hass, H. Ehrenreich, and B. Velický, *Phys. Rev. B* **27**, 1088 (1983).
- ²³R. Triboulet, *Rev. Phys. Appl.* **12**, 123 (1977).
- ²⁴A. Compaan and H. J. Trodahl, *Phys. Rev. B* **29**, 793 (1984).
- ²⁵J. Wagner and M. Cardona, *Solid State Commun.* **48**, 301 (1983).
- ²⁶W. C. Dash and R. Newman, *Phys. Rev.* **99**, 1151 (1955).
- ²⁷D. E. Aspnes and A. A. Studna, *Phys. Rev. B* **27**, 985 (1983).
- ²⁸F. Bechstedt and D. Haus, *Phys. Status Solidi B* **88**, 163 (1978).
- ²⁹M. A. Renucci, J. B. Renucci, R. Zeyher, and M. Cardona, *Phys. Rev. B* **10**, 4309 (1974).
- ³⁰W. Kiefer, W. Richter, and M. Cardona, *Phys. Rev. B* **12**, 2346 (1975).
- ³¹L. Viña and M. Cardona, *Phys. Rev. B* **29**, 6739 (1984).
- ³²J. A. Van Vechten, O. Berolo, and J. C. Woolley, *Phys. Rev. Lett.* **29**, 1400 (1972).
- ³³M. Cardona, *Phys. Rev.* **129**, 69 (1963).